

## Rate of Enolate Formation Is Not Very Sensitive to the Hydrogen Bonding Ability of Donors to Carboxyl Oxygen Lone Pair Acceptors; A Ramification of the Principle of Non-Perfect Synchronization for General-Base-Catalyzed Enolate Formation

Zhenlin Zhong, Timothy S. Snowden, Michael D. Best, and Eric V. Anslyn\*

Contribution from the Department of Chemistry and Biochemistry, 1 University Station, A5300, The University of Texas at Austin, Austin, Texas 78712

Received October 28, 2003; E-mail: anslyn@ccwf.cc.utexas.edu

**Abstract:** Two series of structures (**1** and **2**) possessing intramolecular hydrogen bonds to the lone-pair electrons of carbonyl oxygens have been examined to reveal the influence of the  $pK_a$  of the hydrogen-bond donor on the rate of general-base-catalyzed enolate formation. The geometry of the hydrogen bonds is well accepted to be appropriate for intramolecular hydrogen-bond formation. Yet, as revealed by Brønsted plots, both series show very little dependence of the rate of enolate formation on the hydrogen-bond donor ability. The intramolecular hydrogen bonds give rate enhancements only on the order of 10–100-fold, and corrected Brønsted  $\alpha$ -values are slightly below 0.1. The results can be understood by interpreting them in light of the Principle of Non-Perfect Synchronization. The results are consistent with the proton transfer occurring through an asynchronous transition state with the developing negative charge localized on carbon. We postulate that catalysts of enolate formation will be most effective if the binding groups are focused on stabilizing negative charge that is forming on the enolate carbon rather than on the enolate oxygen.

Many enzymes efficiently deprotonate  $\alpha$ -carbon carbonyl acids that possess  $pK_a$ s in the vicinity of 20 or higher.<sup>1</sup> This is done with general-base catalysis at the enzyme active sites with bases having  $pK_a$ s near 7.0. There is a kinetic barrier that must be overcome in these reactions, as well as a large thermodynamic unfavorability that must be counteracted.<sup>2</sup>

The kinetic barrier is associated with the well-documented difficulty in deprotonating carbon acids. The rate of deprotonation of carbon acids often has little correlation with the exergonic or endergonic nature of the deprotonation, and the rates are lower than would be expected on the basis of their acidities relative to oxygen and nitrogen acids.<sup>3</sup> This is due to the difficulty in forming the hydrogen bond between the base and the carbon acid proton that is required prior to deprotonation.<sup>4</sup> It is also due to a lack of delocalization in the transition state of the negative charge that is being created on the oxygen of the ultimate enolate by a manifestation of the Principle of Non-Perfect Synchronization.<sup>5</sup>

The thermodynamic unfavorability for deprotonating a carbon acid at neutral pH results from the large difference in the  $pK_a$  of the acid relative to the pH in which an enzyme operates. It has been postulated that metal chelation<sup>6</sup> or low-barrier hydrogen

bonds<sup>7</sup> stabilize the conjugate base (enolate) of the carbon acids, thereby lowering the  $pK_a$  of the acid such that the enolate is accessible when bound in the enzyme active site.<sup>8</sup> To enhance the rate of deprotonation, the same interactions could stabilize the transition state for deprotonation.

When one examines the crystal structures of a variety of enolase and racemase enzymes, as well as other enzymes that catalyze reactions involving enolates, hydrogen bonds to the

- (1) Tanner, M. E. *Acc. Chem. Res.* **35**, **2002**, *35*, 237. Babbitt, P. C.; Hasson, M. S.; Wedekind, J. E.; Palmer, D. R. J.; Barrett, W. C.; Reed, G. H.; Rayment, I.; Ringe, D.; Kenyon, G. L.; Gerlt, J. A. *Biochemistry* **1996**, *35*, 16489.
- (2) Gerlt, J. A.; Kozarich, J. W.; Kenyon, G. L.; Gassman, P. G. *J. Am. Chem. Soc.* **1991**, *113*, 9667.
- (3) Eigen, M. *Proceedings of Nobel Symposium*; Almqvist and Wisksell: Stockholm; 1967, p 245.

- (4) For a few examples, see: Kresge, A. J. *Can. J. Chem.* **1974**, *52*, 1897. Hine, J. *Adv. Phys. Org. Chem.* **1977**, *15*, 1. Delbecq, F. *J. Org. Chem.* **1984**, *49*, 4838. Murray, C. J.; Jencks, W. P. *J. Am. Chem. Soc.* **1990**, *112*, 1880. Bell, R. P.; Grainger, S. I. *J. Chem. Soc., Perkin Trans. 2* **1976**, 1367. Bordwell, J. G.; Boyle, W. J. *J. Am. Chem. Soc.* **1972**, *94*, 3907. Bernasconi, C. F.; Ali, M.; Gunter, J. C. *J. Am. Chem. Soc.* **2003**, *125*, 151. Yao, X.; Gold, M. A.; Pollack, R. M. *J. Am. Chem. Soc.* **1999**, *121*, 6220. Bernasconi, C. F.; Moreira, J. A.; Huang, L. L.; Kittredge, K. W. *J. Am. Chem. Soc.* **1999**, *121*, 1674. Nevy, J. B.; Hawkinson, D. C.; Blotny, G.; Yao, X.; Pollack, R. M. *J. Am. Chem. Soc.* **1997**, *119*, 12722. Bernasconi, C. F.; Wenzel, P. J. *J. Am. Chem. Soc.* **1996**, *118*, 11446. Stefanidis, D.; Bunting, J. W. *J. Am. Chem. Soc.* **1991**, *113*, 991.
- (5) Bernasconi, C. F. *Adv. Phys. Org. Chem.* **1992**, *27*, 119.
- (6) Guthrie, J. P.; Kluger, R. *J. Am. Chem. Soc.* **1993**, *115*, 11569.
- (7) Gilli, P.; Valerio, B.; Ferretti, V.; Gilli, G. *J. Am. Chem. Soc.* **1994**, *116*, 909. Hibbert, F.; Emsley, J. *Adv. Phys. Org. Chem.* **1990**, *26*, 255.
- (8) For some examples in the last five years, see: Basran, J.; Patel, S.; Sutcliffe, M. J.; Scrutton, N. S. *J. Biol. Chem.* **2001**, *276*, 6234. Neidhart, D.; Wei, Y.; Cassidy, C.; Lin, J.; Cleland, W. W.; Frey, P. A. *Biochemistry* **2001**, *40*, 2439. Lin, J.; Frey, P. A. *J. Am. Chem. Soc.* **2000**, *122*, 11258. Ha, N.-C.; Kim, M.-S.; Lee, W.; Choi, K. Y.; Oh, B.-H. *J. Biol. Chem.* **2000**, *275*, 41100. Cassidy, C. S.; Lin, J.; Tobin, J. B.; Frey, P. A. *Bioorg. Chem.* **1998**, *26*, 213. Mock, W. L.; Morsch, L. A. *Tetrahedron* **2001**, *57*, 2957. Cleland, W. W. *Arch. Biochem. Biophys.* **2000**, *382*, 1. Cleland, W. Wallace; Frey, P. A.; Gerlt, J. A. *J. Biol. Chem.* **1998**, *273*, 25529. Poi, M. J.; Tomaszewski, J. W.; Yuan, C.; Dunlap, C. A.; Andersen, N. H.; Gelb, M. H.; Tsai, M.-D. *J. Mol. Biol.* **2003**, *329*, 997. Cui, Q.; Karplus, M. *J. Phys. Chem.* **2002**, *B* *106*, 7927. Stratton, J. R.; Pelton, J. G.; Kirsch, J. F. *Biochemistry* **2001**, *40*, 10411. Neidhart, D.; Wei, Y.; Cassidy, C.; Lin, J.; Cleland, W. W.; Frey, P. A. *Biochemistry* **2001**, *40*, 2439.

carbonyl oxygens are found.<sup>9</sup> In fact, in the case of mandelate racemase, a hydrogen bond to the enolate is postulated to be part of the catalytic power that lowers the  $pK_a$  by 25 units,<sup>10</sup> and several investigators have debated whether a low-barrier hydrogen bond may form in the reaction catalyzed by this enzyme.<sup>11</sup>

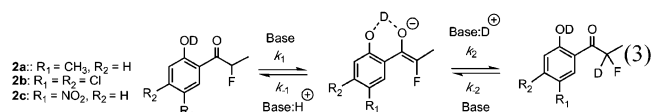
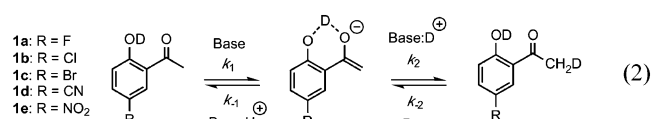
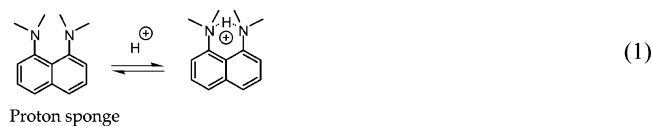
We have examined synthetic model systems and found that hydrogen bonding to the lone-pair electrons of oxygens of  $\alpha$ -carbon acids results in only a small  $pK_a$  lowering,<sup>12</sup> while hydrogen bonding to the  $\pi$ -system of the carbonyl in  $\alpha$ -carbon acids imparts a markedly larger  $pK_a$  lowering.<sup>13</sup> These studies solely involved  $pK_a$  measurements and therefore were tests of the ability of hydrogen bonds to counteract the thermodynamic unfavorability for deprotonation at neutral pH.

Herein, we describe a test of the ability of hydrogen bonds to carbonyl oxygen lone pairs to enhance the rates of enolate formation. We find only a small rate enhancement for enolate formation and a very small Brønsted  $\alpha$ -value. This indicates that the sensitivity of the enolate formation rate constant on the acidity of the hydrogen bond donor is minimal. We interpret the results in light of the Principle of Non-Perfect Synchronization<sup>5</sup> and conclude that hydrogen bonds to oxygen lone-pair electrons in carbonyl  $\alpha$ -carbon acids has little effect on the kinetics of enolate formation. This result may have relevance to the role that hydrogen-bonding plays in enzyme-catalyzed enolate formation.

## Results and Discussion

**Experimental Design.** Proton sponge is a strong base due to the chelation of a proton between both nitrogens (eq 1) and steric repulsion between the lone pair electrons.<sup>14</sup> This geometry is conducive to the formation of strong intramolecular hydrogen bonds, and some researchers have cited this geometry and the strength of the hydrogen bonds to support the notion of low-barrier hydrogen bonds in such structures.<sup>15</sup> Recently, Perrin has shown that protonated proton sponge,<sup>16</sup> and related structures,<sup>17</sup> are not symmetric. Irrespective of whether a low-barrier

hydrogen bond will form or the exact position of the proton, we sought to mimic this hydrogen bonding geometry in a system that can undergo the formation of an enolate. Therefore, we designed the series of compounds designated by **1** and **2** (eqs 2 and 3). Deprotonation of the  $\alpha$ -hydrogens of **1** or **2** by a base creates an enolate, which can be protonated by a proton source, and in our case we used deuterated solvents and/or deuterated buffers. These buffers and solvents rapidly scramble deuterons with the phenyl-OH protons, deuterating these positions as shown with **1** and **2**.

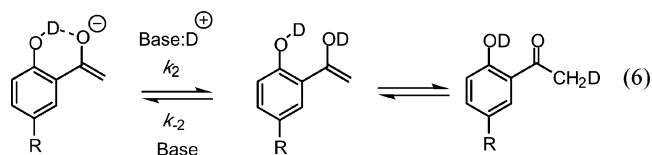


The rate-determining step of general-base-catalyzed enolization of carbonyls is known to be deprotonation to form the enolate,<sup>18</sup> and we verified this in our systems (see below). Following the rate of hydrogen to deuterium scrambling at the  $\alpha$ -carbon gives the rate law in eq 4. With an excess of the conjugate acid of the general-base catalyst in solution, the expression simplifies to that given in eq 5, where the rate constant solely reflects the rate of deprotonation.

$$\text{rate} = k_1 k_2 [\mathbf{1} \text{ or } \mathbf{2}] [\text{base}] [\text{base:D}^+] / (k_{-1} [\text{base}] + k_2 [\text{base:D}^+]) \quad (4)$$

$$\text{rate} = k_1 [\mathbf{1} \text{ or } \mathbf{2}] [\text{base}] \quad (5)$$

However, after enolate formation, the kinetic site of protonation is the oxygen of the enolate, and tautomerization gives the keto form (eq 6).<sup>19</sup> Yet, protonation and deprotonation at oxygen is much faster than at carbon,<sup>19</sup> and therefore the tautomerization reaction occurs faster than the first deprotonation and does not affect the kinetics.

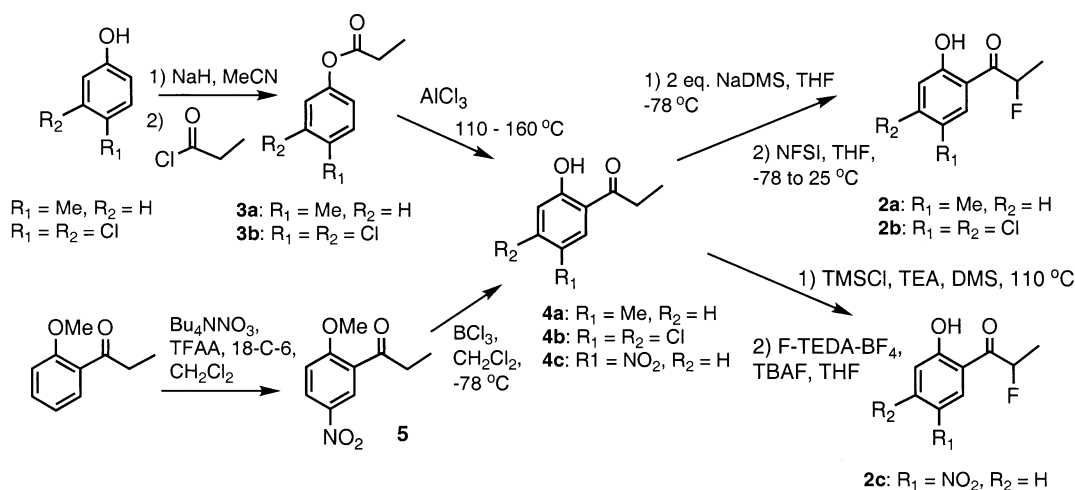


To study the influence of the hydrogen bond donor to the carbonyl oxygen on the rate of carbon acid deprotonation, we required a general-base catalyst that could operate at a pH below all the  $pK_a$ s of the phenol hydrogen-bond donors. We choose

- (9) As a few examples: Vovk, P.; Engst, S.; Eder, M.; Ghisla, S. *Biochemistry* **1998**, *37*, 1848. Wu, W.-J.; Anderson, V. E.; Raleigh, D. P.; Tonge, P. J.; *Biochemistry* **1997**, *26*, 22211. Xiang, H.; Lusong, L.; Taylor, K. L.; Dunaway-Mariano, D. *Biochemistry* **1989**, *28*, 7638.
- (10) Chiang, Y.; Kresge, A. J.; Pruszyński, P.; Schepp, N. P.; Wirz, J. *Angew. Chem., Int. Ed. Engl.* **1990**, *29*, 792.
- (11) Kenyon, G. L.; Gerlt, J. A.; Petsko, G. A.; Kozarich, J. W. *Acc. Chem. Res.* **1995**, *28*, 178.
- (12) Kelly-Rowley, A. M.; Lynch, V. M.; Anslyn, E. V. *J. Am. Chem. Soc.* **1995**, *117*, 3438.
- (13) Snowden, T. S.; Bisson, A. P.; Anslyn, E. V. *J. Am. Chem. Soc.* **1999**, *121*, 6324. Snowden, T. S.; Bisson, A. P.; Anslyn, E. V. *Bioorg. Med. Chem.* **2001**, *9*, 2467.
- (14) Bienko, A. J.; Latajka, Z.; Sawka-Dobrowolska, W.; Sobczyk, L.; Ozeryanski, V. A.; Pozharskii, A. F.; Grech, E.; Nowicka-Scheibe, J. *J. Chem. Phys.* **2001**, *119*, 4313. Howard, S. T. *J. Am. Chem. Soc.* **2000**, *122*, 8238. Perakyla, M. *J. Org. Chem.* **1996**, *61*, 7420.
- (15) Frey, P. A. *Science* **1995**, *269*, 104. Alder, R. W.; Goode, N. C.; Miller, N.; Hibbert, F.; Hunte, K. P. P.; Robbins, H. J. *J. Chem. Soc., Chem. Commun.* **1978**, 89. The heteroatom separation distances in LBHB systems involving nitrogen may often be greater than that acceptable where oxygen acts as both donor/acceptor due to the increased van der Waals radii of the nitrogen atoms. However, numerous authors have defined the outer limit of LBHB formation between oxygen donor/acceptor atoms as 2.5 Å. In fact, a sharp increase in hydrogen bond energy arises as O–H–O separation is decreased from 2.52 to 2.42 Å, within which our model falls as predicted by molecular mechanics calculations. LBHBs are also believed to exist in some  $\beta$ -diketones involved in keto–enol equilibria. Such compounds are directly comparable to our system in donor–acceptor atoms, geometry, and heteroatom separation.
- (16) Perrin, C. L.; Ohta, B. K. *J. Am. Chem. Soc.* **2001**, *123*, 6520.
- (17) Perrin, C. L.; Ohta, B. K. *Bioorg. Chem.* **2002**, *30*, 3. Perrin, C. L. *J. Am. Chem. Soc.* **1992**, *114*, 8550.

- (18) For a system very similar to that studied herein that both indicates the rate-determining step for enolization and shows a transition state imbalance similar to that we discuss herein, see: Yao, X.; Gold, M. A.; Pollack, R. M. *J. Am. Chem. Soc.* **1999**, *121*, 6220.
- (19) Kresge, A. J. *Acc. Chem. Res.* **1975**, *8*, 354. Kresge, A. J. *Pure Appl. Chem.* **1991**, *63*, 213.

Scheme 1



imidazole/imidazolium chloride for our studies in methanol/water at  $\text{pD}$  of 5.8 and a 1:1 ratio of imidazole/imidazolium triflate in acetonitrile. These low  $\text{pH(D)}$  values relative to the phenols in **1** and **2** ensured that the phenols were primarily in their acidic form during the kinetic analyses.

We measured rate enhancements and created Brønsted plots in both 80% methanol/20% water (pure water was not used for solubility reasons) and dry acetonitrile as the solvents. In the protic solvent system, the effect of the hydrogen bond donors on the rate of enolate formation was not expected to be as dramatic as in the lower dielectric aprotic acetonitrile solvent. Further, in our previous studies of the thermodynamics for hydrogen bonding on enolate formation,<sup>12,13</sup> we used acetonitrile, and hence we again examined acetonitrile for comparison to our earlier studies.

The reason we choose two series of structures (**1** and **2**) for this study is related to the  $\text{pK}_a$  of the enol form of the reactants. First, the  $\text{pK}_a$  of the enol forms of **1** are expected to be in the range determined by Kresge for acetophenone (11.7, although it would be raised by approximately 1 unit in the methanol/water mixture used; see below).<sup>20</sup> The  $\text{pK}_a$  of the enol is the proper  $\text{pK}_a$  to consider when determining the difference between the  $\text{pK}_a$  of the hydrogen-bond-donating phenol and the  $\text{pK}_a$  of the conjugate acid of the hydrogen bond acceptor enolate. The closer these  $\text{pK}_a$  values, the greater the sharing of the hydrogen in the hydrogen bond formed between the donor and acceptor.<sup>21</sup> The  $\text{pK}_a$ s of the phenols used in this study were between 8 and 12 in methanol/water (see below), near or below the  $\text{pK}_a$  of the enol forms of the reactants represented by **1**. Therefore, we desired a series of structures with lower enol  $\text{pK}_a$  values. In this regard, we synthesized a small number of structures represented by **2**. Although the exact lowering imparted to the enol  $\text{pK}_a$  values from the  $\alpha$ -fluoro group was not determined in our study, it was expected to be in the range of 2 to 3  $\text{pK}_a$  units. This estimate derives from the lowering of the  $\text{pK}_a$  values of carboxylic acids imparted by  $\alpha$ -fluoro substitution. Therefore, the estimated  $\text{pK}_a$  values of the enol forms of **2** are in the range of 9 to 10, which overlaps with the  $\text{pK}_a$  values of the hydrogen

bonding phenol groups. Hence, one may expect a greater extent of hydrogen atom sharing in the hydrogen bond formed in the enolates of **2** than in the enolates of **1**. Therefore, with **2** we expected larger  $\alpha$ -values, because the  $\alpha$ -value is often considered to be indicative of the extent of proton transfer in the transition state. Part of our study set out to determine what effect this difference in hydrogen bonding in the enolates has on the rates of enolate formation.

**Synthesis.** All structures represented by **1** were commercially available, and the corresponding methyl ethers were made using  $\text{CH}_3\text{I}$  and  $\text{K}_2\text{CO}_3$  in acetone (see Experimental Section). Synthesis of the series **2** structures was more involved (Scheme 1). The phenols ( $R = \text{Cl}$  or  $\text{Me}$ ) were first acetylated, followed by a Fries rearrangement with added  $\text{AlCl}_3$  at elevated temperatures (**4**). With  $R = \text{NO}_2$ , the OH of hydroxyacetophenone was first protected, followed by nitration of the aromatic ring with  $\text{Bu}_4\text{NNO}_3$  (**5**), and finally deprotected to make **4c**. The fluorination followed two different routes also. In the preparation of **3a** and **3b**, the enolates of **4a** and **4b** were allowed to react with *N*-fluorobenzene sulfonamide. In the case of **3c**, the enolate from **4c** was stirred with Selectfluor.

**Kinetics.** Before creating Brønsted plots to decipher the rate enhancement for enolate formation and the sensitivity of the reaction to the hydrogen bond donor, we set out to explore the mechanism of deuterium exchange. As discussed above, on the basis of literature precedent we anticipated general-base catalysis by the added buffer.<sup>22</sup> Figure 1 confirms this expectation in the 4/1 methanol/water mixture with **1** ( $R = \text{Cl}$ ). Part A shows the first-order dependence upon the imidazole component of the buffer, and Part B shows the  $\text{pD}$  versus rate profile for various ratios of imidazolium and imidazole. This latter graph has the characteristic shape indicative of general-base catalysis with a base whose conjugate acid possesses a  $\text{pK}_a$  of near 7 ( $\text{pK}_a$  of imidazolium is 6.95).<sup>23</sup> As a separate test, Figure 2 shows a plot of the rate constant for H to D exchange with **1** ( $R = \text{CN}$ ) as a function of buffer concentration. Whereas Figure 1a has a near zero  $y$ -intercept, Figure 2 has a small but nonzero intercept. Apparently, there is slight solvent catalysis with  $R = \text{CN}$  relative to  $R = \text{Cl}$ .

(20) Pruszyński, P.; Chiang, Y.; Kresge, A. J.; Schepp, N. P.; Walsh, P. A. *J. Phys. Chem.* **1986**, *90*, 3760.

(21) As the  $\text{pK}_a$  of the hydrogen bond donor HA approaches that of the conjugate acid of the hydrogen bond acceptor B, the energy wells for placing the hydrogen on A or B become closer in energy.

(22) Schowen, K. B.; Limbach, H. H.; Denisov, G. S.; Schowen, R. L. *Biochim. Biophys. Acta*, **2000**, *1458*, 43.

(23) Varnagy, K.; Savano, I.; Agoston, K.; Liko, Z.; Sueli-Vargha, H. *J. Chem. Soc., Dalton Trans.*, **1994**, *20*, 2939.

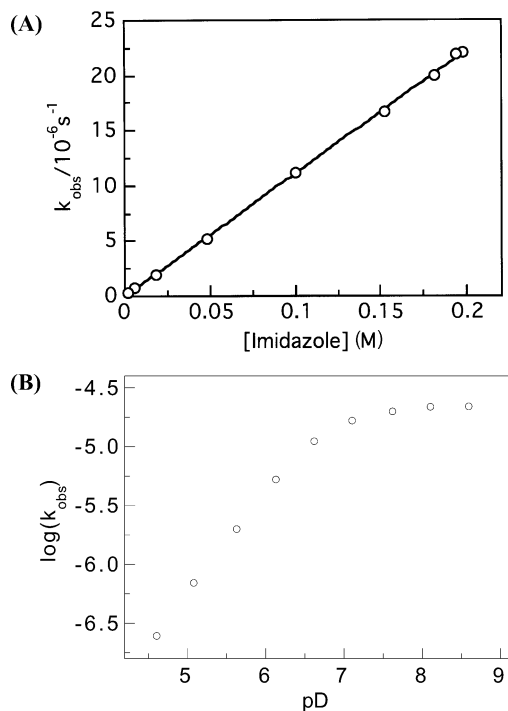


**Figure 1.** Influence of the free base concentration (A) and pD (B) on the rate constant of H/D exchange of **1** (R = Cl) in 4:1 CD<sub>3</sub>OD/D<sub>2</sub>O (v/v) buffered with imidazole–imidazolium chloride 99:1 to 1:99 with a total concentration of 200 mM. [I] = 20 mM.

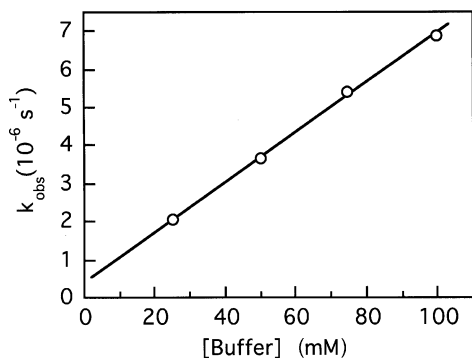


**Figure 2.** Influence of buffer concentration on the rate constant of H/D exchange of 25 mM of **1** (R = CN) in 4:1 CD<sub>3</sub>OD/D<sub>2</sub>O (v/v) buffered with imidazole–imidazolium chloride at pD 5.83.

With this information in hand, it was appropriate to explore Brønsted plots. The form of the Brønsted equation we used is given in eq 7, where  $\alpha$  gives a rough measurement of the extent of proton transfer at the transition state from the hydrogen-bond-donating phenol groups. The  $k_{\text{obs}}$  values are the rate constants for  $\alpha$ -hydrogen exchange, and the  $\text{p}K_{\text{a}}$  values are for the phenol groups in the solvent systems used.

$$\log(k_{\text{obs}}) = -\alpha\text{p}K_{\text{a}} + C \quad (7)$$

Figures 3A and 3B show the Brønsted plots generated for series **1** in 4/1 CD<sub>3</sub>OD/D<sub>2</sub>O and acetonitrile, respectively, along with analogous plots of the methyl ether-protected versions of each **1** structure. Because the solvent system and/or buffer is deuterated in each study, the phenols of **1** are rapidly exchanged with deuterium. Hence, the hydrogen bonds formed between the enolates and phenols involve deuterium. This does not affect the conclusions of our studies because hydrogen bonds with

**Table 1.**  $\text{p}K_{\text{a}}$  Values of the Species **1** in the Two-Solvent Systems Studied

solvent	R				
	–NO <sub>2</sub> (1e)	–CN (1d)	–Br (1c)	–Cl (1b)	–F (1a)
4:1 MeOH/H <sub>2</sub> O	7.98	8.83	10.79	10.90	11.46
CH <sub>3</sub> CN	19.55	21.25	24.56	24.91	25.64

deuterium are actually stronger than with hydrogen.<sup>24</sup> Further, it does not have a dramatic influence on the slopes of the Brønsted plots relative to hydrogen, because the slope reflects a difference in hydrogen bond strengths between the various phenols and every phenol is deuterated in the study.

To create the Brønsted plots in methanol/water and acetonitrile, the  $\text{p}K_{\text{a}}$  values of the phenols were measured in these two solvent systems. In 4/1 methanol/water, simple potentiometric titrations with NaOH were performed, followed by analysis of the extent of deprotonation with a UV/vis spectrum. Each phenol  $\text{p}K_{\text{a}}$  is raised in the 4/1 methanol/water mixture by approximately 1 unit relative to water. The  $\text{p}K_{\text{a}}$  values in acetonitrile are 10–14 units higher. Table 1 lists the  $\text{p}K_{\text{a}}$  values found for the series **1** compounds in the two-solvent systems used.

In acetonitrile, the  $\text{p}K_{\text{a}}$ s of the phenols were determined by mixing the phenol with various indicators of known  $\text{p}K_{\text{a}}$ s (see Experimental Section). First, aliquots of tetrabutylammonium hydroxide were added to the indicators and the phenols separately to obtain spectra of the acids and their conjugate bases. Next, the phenols and indicators were mixed together, and the composite spectra were recorded for several additions of NBu<sub>4</sub>OH; the ratio of acids to conjugate bases was determined for each addition of NBu<sub>4</sub>OH. The phenol  $\text{p}K_{\text{a}}$  values were determined by comparing the ratio of the acid to conjugate base forms of the phenols and the indicators (see Table 1).

The rate enhancements between the series of structures depicted in Figure 3A is only on the order of 1 log unit, a factor of 10. This is a small rate enhancement from an intramolecularly coordinated hydrogen bond.<sup>25</sup> Further, the  $\alpha$ -values of the two plots shown in Figure 3A are only 0.24 and 0.15. The  $\alpha$ -values for the series **1** phenols reflect the sensitivity of the rate constant for enolate formation to the hydrogen-bond-donating ability of the phenols and to the placement of the substituent on the aromatic ring. The sensitivity of enolate formation for the methyl ether-protected versions of **1** derives solely from the substituent effects on the phenyl ring. Therefore, to achieve an  $\alpha$ -value that only reflects the extent to which hydrogen bonding affects the rate of the enolate formation, one needs to subtract these values. This results in a very small value of 0.09. This value was reproducibly greater than zero but is indeed approaching zero. In other words, there is little sensitivity of the rate constant for enolate formation on the hydrogen-bond-donating ability of a donor coordinated to a carbonyl oxygen lone pair.

To see if a greater sensitivity for facilitating enolate formation by hydrogen bonding is found in an aprotic solvent, acetonitrile was used. Figure 3B shows the analogous plots to Figure 3A, except with acetonitrile as the solvent. Indeed, the rate enhancement imparted by the hydrogen bonding phenols is greater, being a factor of around 20 to 100 on average. However, the difference

(24) For a recent study that exploits this fact, see: Shi, Z.; Krantz, B. A.; Kallenbach, N.; Sosnick, T. R. *Biochemistry* **2002**, *41*, 2120.

(25) Hartwell, E.; Hodgson, D. R. W.; Kirby, A. J. *J. Am. Chem. Soc.* **2000**, *122*, 9326.



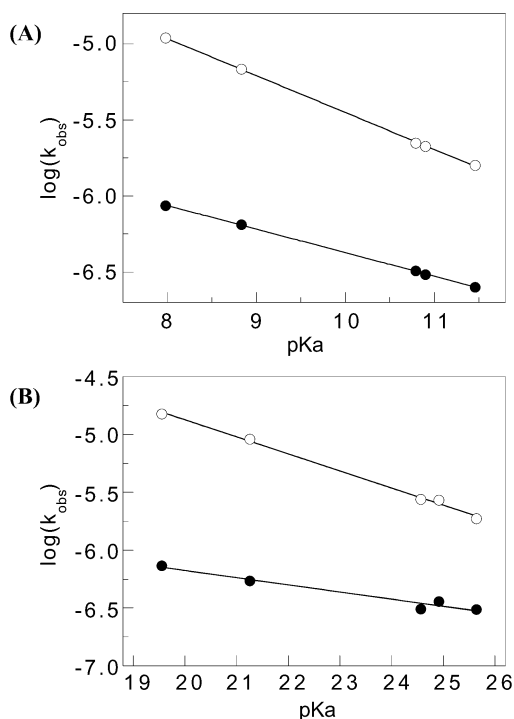


**Figure 3.** Brønsted plots in (A) 4:1  $\text{CD}_3\text{OD}/\text{D}_2\text{O}$  (v/v) buffered with 100 mM imidazole at pD 5.83 (slopes are  $-0.242$  and  $-0.154$ , respectively) and (B)  $\text{CD}_3\text{CN}$  buffered with 150 mM imidazole- $d_2$  and 150 mM imidazolium- $d_3$  triflate (slopes are  $-0.148$  and  $-0.062$ , respectively). Open circles are for **1**, and closed circles are for methyl ether-protected versions of **1**. Concentrations of reactants were 20 mM. Since there is no phenolic OH in the ethers, it is plotted to the same  $pK_a$  scale of **1**.

in the  $\alpha$ -values between the phenols and the methyl ether-protected versions is the same as was found for  $\text{MeOH}/\text{H}_2\text{O}$  (0.09). Therefore, although the rate enhancement is larger in acetonitrile, the sensitivity for enolate formation on the acidity of the hydrogen bond donors is about the same as in the protic solvent.

To check if lowering the  $pK_a$  of the enol would impart a greater sensitivity to the hydrogen bond donor ability of the phenol donor, we analyzed the series **2** compounds. The  $pK_a$  of the conjugate acids of the enolates (enols) are closer to the  $pK_a$ s of the donor phenols (see Design Criteria). The hypothesis was that the decreased disparity between the  $pK_a$ s might enhance the  $\alpha$ -values because more sharing of the hydrogen between the donor and acceptor will occur in the enolate. Because the series **2** structures are more challenging to synthesize, only three were initially made to get an estimate for the  $\alpha$ -value.

Once again, the differences between the rate constants for enolate formation are small (Figure 4). Because of the small differences in rate constants with these three structures, we did not synthesize more analogues, nor did we study the methyl-protected versions. Similarly, we did not pursue an accurate determination of the  $pK_a$  values of these phenols in acetonitrile but instead simply used their  $pK_a$ s as determined in water. This gave an  $\alpha$ -value of 0.24 (Figure 4). This  $\alpha$ -value is similar to those for the compounds represented as **1**, meaning that the fluorine substitution did not make a large difference. In fact, in acetonitrile the  $\alpha$ -value would be even lower because the  $pK_a$  scale is wider. However, because it was clear that the  $\alpha$ -values for series **2** did not lead to a dramatic increase in the sensitivity to the hydrogen bond donor, the extra labor to make this Brønsted plot more accurate did not seem warranted.

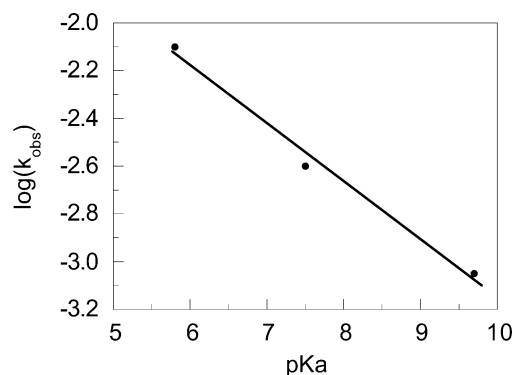


**Figure 4.** Brønsted plot for **2**. Concentrations of **2** were 20 mM.  $\text{CD}_3\text{CN}$  was buffered with 150 mM imidazole- $d_2$  and 150 mM imidazolium- $d_3$  triflate (slope is  $-0.24$ ).

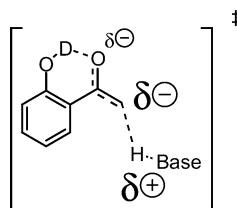
**Interpretation of the Results.** One is left wondering why the rate enhancements imparted by the intramolecular hydrogen bonding are so small and why the rate of general-base catalyzed enolate formation is so insensitive to the hydrogen bonding ability of the phenol donors. Kirby has previously noted that intramolecular general-acid catalysis via hydrogen bonds is particularly inefficient relative to intramolecular nucleophilic catalysis.<sup>26</sup> Geometrical considerations and the lack of the ability to form strong intramolecular hydrogen bonds at the transition states were considered the basis for the general lack of efficiency in those studies. However, as summarized earlier, our hydrogen bond geometry was modeled after that present in proton sponge and has been postulated to support low-barrier hydrogen bond formation. Hence, we sought an alternative explanation for the observed low efficiency in our system. We postulate that the answer resides in the Principle of Non-Perfect Synchronization.<sup>5</sup>

This principle postulates that the delocalization of negative charge onto the oxygen of an enolate in the transition state for deprotonation of  $\alpha$ -carbon acids lags significantly behind the extent of deprotonation. The principle was put forth to explain why the rates of deprotonation of many carbon acids do not correlate with their acidities. This is particularly so with  $\alpha$ -hydrogens to nitro groups, leading to what is known as the nitro alkane anomaly. Yet, it is a general phenomenon for carbon acids. The principle stems from the fact that deprotonation of the  $\alpha$ -carbon moves a light atom (hydrogen), while subsequent rearrangement of the C–C and C–O bond lengths necessary for the delocalization of charge onto oxygen lags behind.

Our study supports this notion in intramolecular general-acid-catalyzed enolate formation. The intramolecular hydrogen bonds in series **1** and **2** to the developing enolate oxygen were found to have little effect on the rate of deprotonation. Whereas, if significant negative charge were developing on the enolate oxygen, hydrogen bonding to that oxygen would be expected to give a much larger extent of proton transfer. How much more transfer is an important question to address, and we are currently seeking an answer with other model systems. Yet, clearly a proton transfer of only around 9% (0.09  $\alpha$ -value) at the transition state from a series of phenols whose  $pK_a$ s are below that of the conjugate acid of the enolate acceptor indicates very little charge on the oxygen. Moreover, the low  $\alpha$ -value is indicative of a slight increase in hydrogen bonding and with very little proton transfer.<sup>27</sup> Hence, we envision a transition state with an activated

(26) Kirby, A J. *Acc. Chem. Res.* **1997**, *30*, 290.

complex as shown below, where little negative charge is on the ultimate enolate oxygen and most of the negative charge resides on the carbon.



The study presented here and the explanation based upon the principle of non-perfect synchronization give insight into enzymatic catalysis of  $\alpha$ -carbon deprotonations and a lesson for the creation of artificial enzymes for enolate formation. It suggests that very little catalytic power for deprotonation of  $\alpha$ -carbons will be derived from hydrogen bonding to the carbonyl oxygen lone pairs. Instead, greater catalysis may be achieved by focusing stabilizing forces on the negative charge that is being primarily created on the  $\alpha$ -carbon during the deprotonation. Alternatively, coordination of more powerful electrophiles than traditional hydrogen bonds such as metals may alter the structure of the transition state for deprotonation, allowing more delocalization to the carbonyl oxygen and altering the non-perfect synchronization of the delocalization in the enolate at the transition state. Last, on the basis of some of our previous studies,<sup>12,13</sup> placement of the hydrogen bond donors oriented at the  $\pi$ -system of the enolate, rather than at oxygen lone pair electrons, may impart both a markedly greater rate enhancement and a larger sensitivity to an intramolecularly coordinated hydrogen bond. This hypothesis is currently under investigation in our laboratories.

## Experimental Section

**General.** UV–vis measurements were performed on a Beckman DU-640 UV–vis spectrophotometer. <sup>1</sup>H NMR spectra were recorded at 400 MHz on a Varian Mercury 400 spectrometer. pH measurements were performed on an Orion 720A pH meter with a glass electrode. Anhydrous acetonitrile for the acidity studies was purchased from EM Science (OmniSolv, containing 8.5 ppm of water). Compounds **1a–c** were commercially available. Compounds **1d**<sup>28</sup> and **1e**<sup>29</sup> and the methyl ether-protected version of **1c**<sup>30</sup> were synthesized according to the literature. Imidazole-*d*<sub>2</sub> was prepared by treating imidazole in D<sub>2</sub>O under reflux overnight under argon followed by evaporation of the solvent and drying under vacuum. Imidazolium-*d*<sub>3</sub> triflate was prepared from imidazole-*d*<sub>2</sub> by addition of 1 equiv of HOTf in D<sub>2</sub>O followed by evaporation of the solvent and drying under vacuum. All other chemicals were purchased from Aldrich and used without further purification. All measurements were done at 25 °C.

**Syntheses of 3-Substituted 6-Methoxyacetophenones.** A mixture of a 3-substituted 6-hydroxyacetophenone (**1a**, **1b**, **1d**, or **1e**) (10 mmol) and anhydrous K<sub>2</sub>CO<sub>3</sub> (4.1 g, 30 mmol) in acetone (20 mL) was stirred for 1 h at room temperature under argon. Iodomethane (0.81 mL, 13 mmol) was added in one portion. The reaction mixture was stirred for 15 h and checked by TLC (silica gel, CH<sub>2</sub>Cl<sub>2</sub>). If the reaction was not completed, additional iodomethane (0.2 mL) was added, and the reaction was continued for an additional 3 h. After the reaction was completed, the solvent was removed by evaporation. Ether (40 mL) and water (40 mL) were added. The ethereal phase was washed with 5% aqueous

K<sub>2</sub>CO<sub>3</sub> solution (20 mL) and water (2 × 20 mL), dried over MgSO<sub>4</sub>, evaporated to dryness, and dried in a vacuum to yield the title compounds in 97–99% yield. **R = F:** <sup>1</sup>H NMR (400 MHz, CDCl<sub>3</sub>, TMS)  $\delta$  7.45 (dd, *J* = 8.9, 3.3 Hz, 1H), 7.18–7.13 (m, 1H), 3.90 (s, 3H), 6.93 (dd, *J* = 8.9, 4.1 Hz, 1H), 2.61 (s, 3H); <sup>13</sup>C NMR (100 MHz, CDCl<sub>3</sub>)  $\delta$  198.27, 157.77, 155.26 (d, *J* = 24 Hz), 128.74 (d, *J* = 5 Hz), 119.95 (d, *J* = 23 Hz), 116.36 (d, *J* = 24 Hz), 112.87 (d, *J* = 7 Hz), 55.95, 31.64; HRMS (CI) *m/z* 169.0656 (calcd for C<sub>9</sub>H<sub>10</sub>O<sub>2</sub>F (M + H<sup>+</sup>) 169.0665). **R = Cl:** <sup>1</sup>H NMR (400 MHz, CDCl<sub>3</sub>, TMS)  $\delta$  7.69 (d, *J* = 2.7 Hz, 1H), 7.40 (qd, *J* = 8.9, 2.8, 0.7 Hz, 1H), 6.91 (d, *J* = 8.9 Hz, 1H), 3.91 (s, 3H), 2.60 (s, 3H); <sup>13</sup>C NMR (100 MHz, CDCl<sub>3</sub>)  $\delta$  198.28, 157.40, 133.10, 129.94, 129.09, 128.85, 113.05, 55.81, 31.69; HRMS (CI) *m/z* 185.0361 (calcd for C<sub>9</sub>H<sub>10</sub>O<sub>2</sub>Cl (M + H<sup>+</sup>) 185.0369). **R = CN:** <sup>1</sup>H NMR (400 MHz, CDCl<sub>3</sub>, TMS)  $\delta$  8.02 (d, *J* = 2.1 Hz, 1H), 7.75 (dd, *J* = 8.7, 2.2 Hz, 1H), 7.07 (d, *J* = 8.9 Hz, 1H), 4.01 (s, 3H), 2.62 (s, 3H); <sup>13</sup>C NMR (100 MHz, CDCl<sub>3</sub>)  $\delta$  197.44, 161.54, 137.09, 134.75, 128.86, 118.20, 112.50, 104.42, 56.06, 31.67; HRMS (CI) *m/z* 176.0714 (Calcd for C<sub>10</sub>H<sub>10</sub>NO<sub>2</sub> (M + H<sup>+</sup>) 176.0712). **R = NO<sub>2</sub>:** <sup>1</sup>H NMR (400 MHz, CDCl<sub>3</sub>, TMS)  $\delta$  8.62 (d, *J* = 3.0 Hz, 1H), 8.36 (dd, *J* = 9.0, 3.0 Hz, 1H), 7.09 (d, *J* = 9.2 Hz, 1H), 4.06 (s, 3H), 2.65 (s, 3H); <sup>13</sup>C NMR (100 MHz, CDCl<sub>3</sub>)  $\delta$  197.20, 162.99, 141.28, 128.74, 128.36, 126.49, 111.90, 56.52, 31.58; HRMS (CI) *m/z* 196.0612 (calcd for C<sub>9</sub>H<sub>10</sub>NO<sub>4</sub> (M + H<sup>+</sup>) 196.0610).

**1-(2-Methoxy-5-nitrophenyl)propan-1-one (5).** To a solution of 1-(2-methoxyphenyl)propan-1-one (2.92 g, 17.8 mmol) in dichloromethane (50 mL) and trifluoroacetic anhydride (17.5 mL, 124 mmol) was added 18-crown-6 (16.5 g, 62.4 mmol) under argon. The solution was stirred rapidly until all crown ether had dissolved (10–20 min); then tetrabutylammonium nitrate (5.415 g, 17.8 mmol) was added and the solution mixed at rt for 3.5 h (progress monitored by TLC). The reaction solution was poured onto saturated aqueous sodium bicarbonate (125 mL) and carefully washed. The aqueous phase was removed and extracted with dichloromethane (3 × 20 mL), and then the combined organics were washed with brine (100 mL), dried over Na<sub>2</sub>SO<sub>4</sub>, vacuum filtered, and concentrated by rotary evaporation at 35 °C. The resulting amorphous yellow solid was purified by flash chromatography (4:1 hexanes/ethyl acetate) affording a cream-colored solid. This was triturated with cold hexanes/EtOAc (99:1) leaving 3.40 g of **5** (91%) as a pure white solid: <sup>1</sup>H NMR (300 MHz, CDCl<sub>3</sub>)  $\delta$  8.45 (d, 1H), 8.24 (dd, 1H), 7.12 (d, 1H), 3.97 (s, 3H), 2.92 (q, 2H), 1.10 (t, 3H); <sup>13</sup>C NMR (75 MHz, CDCl<sub>3</sub>)  $\delta$  200.8, 162.6, 141.2, 128.5, 128.3, 126.1, 111.8, 56.5, 36.9, 8.04; HRMS (CI<sup>+</sup>) calcd for C<sub>10</sub>H<sub>12</sub>NO<sub>4</sub> 210.0766, found 210.0767.

**General Procedure for the Preparation of Phenyl Propanoates.** To a rapidly stirring solution of the substituted phenol (near 80 mmol) in acetonitrile (120 mL) was slowly added powdered sodium hydroxide (near 98 mmol) under argon. After 75 min, propionyl chloride was added (near 91 mmol), turning the solution opaque. After stirring for 16 h at rt, the mixture was poured onto saturated aqueous sodium bicarbonate (125 mL; additional water may have to be added, as salts frequently precipitate from the aqueous phase) and extracted with ethyl acetate (3 × 150 mL). The combined organics were washed with brine (150 mL), dried over Na<sub>2</sub>SO<sub>4</sub>, vacuum filtered, and concentrated by rotary evaporation at 40 °C. The crude product was purified using flash chromatography (commonly 19/1 hexanes/ethyl acetate), affording the products as colorless oils. Yields were typically in the range of 90–95%.

**4-Methylphenyl Propanoate (3a).** The crude product was purified using flash chromatography (99:1 hexanes/ethyl acetate), affording **3a** as a colorless liquid: <sup>1</sup>H NMR (300 MHz, CDCl<sub>3</sub>)  $\delta$  7.10 (dd, 1H), 6.84 (d, 1H), 6.79 (dd, 1H), 2.57 (q, 2H), 2.23 (s, 3H), 2.21 (s, 3H), 1.24 (t, 3H); <sup>13</sup>C NMR (75 MHz, CDCl<sub>3</sub>)  $\delta$  172.9, 148.4, 135.1, 129.7, 121.1, 27.5, 20.7, 8.90.

**3,4-Dichlorophenyl Propanoate (3b).** The crude product was purified using flash chromatography (95:5 hexanes/ethyl acetate), affording **3b** as a clear yellow liquid: <sup>1</sup>H NMR (300 MHz, CDCl<sub>3</sub>)  $\delta$

(27) Abraham, M. H. *Chem. Soc. Rev.* **1993**, 22, 73.

(28) Ellis, G. P.; Shaw, D. J. *Chem. Soc., Perkin Trans. 1* **1972**, 779.

(29) Joshi, S. S.; Singh, H. J. *Am. Chem. Soc.* **1954**, 76, 4993.

7.42 (d, 1H), 7.24 (d, 1H), 6.97 (dd, 1H), 2.57 (q, 2H), 1.24 (t, 3H);  $^{13}\text{C}$  NMR (75 MHz,  $\text{CDCl}_3$ )  $\delta$  172.2, 149.3, 132.7, 130.5, 129.4, 123.8, 121.2, 27.5, 8.80; HRMS ( $\text{Cl}^+$ ) calcd for  $\text{C}_9\text{H}_9\text{O}_2\text{Cl}_2$  218.9980, found 218.9970.

**General Procedure for Preparation of 1-(2-Hydroxyphenyl)propan-1-ones via the Fries Rearrangement.** To the phenylpropanoates (near 14 mmol) in a flame-dried one-neck flask fitted with a condenser and heated to 110 °C was quickly added solid  $\text{AlCl}_3$  (near 15 mmol). The resulting dark material was heated for 90 min, cooled to rt, and taken up in 4 N HCl (50 mL). The aqueous phase was extracted with ether ( $2 \times 50$  mL), and ethyl acetate ( $3 \times 50$  mL), and then the combined organics were washed with 1 N sodium acetate (50 mL) and brine (50 mL). After drying with  $\text{Na}_2\text{SO}_4$ , vacuum filtration, and concentration by rotary evaporation at 40 °C, the crude material was purified by flash chromatography (96/4 hexanes/EtOAc), leaving the product as a white solid (yields typically in the range of 90–95%).

**1-(2-Hydroxy-5-methylphenyl)propan-1-one (4a).** The red amorphous solid was purified by flash chromatography (97:3 hexanes/EtOAc) leaving **4a** as a yellow liquid.  $^1\text{H}$  NMR (300 MHz,  $\text{CDCl}_3$ )  $\delta$  12.2 (s, 1H), 7.53 (d, 1H), 7.28 (dd, 1H), 6.87 (d, 1H), 3.01 (q, 2H), 2.30 (s, 3H), 1.23 (t, 3H); HRMS ( $\text{Cl}^+$ ) calcd for  $\text{C}_{10}\text{H}_{13}\text{O}_2$  165.0916, found 165.0921.

**1-(4,5-Dichloro-2-hydroxyphenyl)propan-1-one (4b).** Reactants were heated at 160 °C for 3 h before cooling to rt. The white solid obtained after workup was purified by flash chromatography (95:5 hexanes/EtOAc), when necessary, leaving **4b** as a white solid:  $^1\text{H}$  NMR (300 MHz,  $\text{CDCl}_3$ )  $\delta$  12.2 (s, 1H), 7.80 (s, 1H), 7.09 (s, 1H), 2.99 (q, 2H), 1.23 (t, 3H);  $^{13}\text{C}$  NMR (75 MHz,  $\text{CDCl}_3$ )  $\delta$  205.5, 160.9, 139.9, 130.5, 122.3, 120.3, 118.6, 31.7, 7.83; HRMS ( $\text{Cl}^+$ ) calcd for  $\text{C}_9\text{H}_7\text{O}_2\text{Cl}_2$  218.9980, found 218.9976.

**1-(2-Hydroxy-5-nitrophenyl)propan-1-one (4c).** To a rapidly stirred  $-78$  °C solution of 1-(2-methoxy-5-nitrophenyl)propan-1-one (**5**) (1.34 g, 6.38 mmol) in dry dichloromethane (20 mL) was added 1 M  $\text{BCl}_3$  in dichloromethane (18 mL, 18 mmol). After being gradually warmed to room temperature over 14 h, the solution was poured onto 1 N sodium acetate (30 mL) and shaken well. The organic phase was separated, and the aqueous phase was extracted with dichloromethane (25 mL). The combined organics were washed with brine (30 mL), dried over sodium sulfate, vacuum filtered, and concentrated by rotary evaporation at 35 °C. The crude solid was purified using flash chromatography (short column; 9:1 hexanes/EtOAc) leaving **4c** as a white solid in 92% yield.  $^1\text{H}$  NMR (300 MHz,  $\text{CDCl}_3$ )  $\delta$  13.0 (s, 1H), 8.75 (d, 1H), 8.34 (dd, 1H), 7.09 (d, 1H) 3.16 (q, 2H), 1.29 (t, 3H);  $^{13}\text{C}$  NMR (75 MHz,  $\text{CDCl}_3$ )  $\delta$  206.5, 167.1, 139.5, 130.8, 126.3, 119.6, 118.0, 31.8, 7.78; HRMS ( $\text{Cl}^+$ ) calcd for  $\text{C}_9\text{H}_7\text{NO}_3$ : 196.0610, found 196.0607.

**1-(4,5-Dichloro-2-hydroxyphenyl)-2-fluoropropan-1-one (2b).** To a  $-78$  °C solution of 1-(4,5-dichloro-2-hydroxyphenyl)propan-1-one (1.45 g, 6.62 mmol) and THF (7.0 mL) in a three-neck flask fitted with an addition funnel was added 1.0 M sodium bis(trimethylsilyl)amide (13.4 mL, 13.4 mmol) rapidly in one portion. The solution was stirred for 90 min at  $-78$  °C under argon, and then *N*-fluorobenzene sulfonamide (2.30 g, 7.29 mmol) dissolved in THF (8.0 mL) was added slowly dropwise. The solution was mixed for 90 min at  $-78$  °C and then was allowed to warm to rt (45–60 min.). Ammonium chloride (1 N, 30 mL) was added, and the aqueous phase was extracted with EtOAc ( $2 \times 25$  mL). The combined organics were washed with brine (30 mL), dried over  $\text{Na}_2\text{SO}_4$ , vacuum filtered, and concentrated by rotary evaporation at 40 °C. The crude oil was purified by flash chromatography (97.3 hexanes/EtOAc), providing 1.08 g (69%) of **2b** as a yellow solid:  $^1\text{H}$  NMR (300 MHz  $\text{CDCl}_3$ )  $\delta$  11.8 (s, 1H), 7.94 (s, 1H), 7.14 (s, 1H), 5.62 (dq, 1H), 1.70 (dd, 3H);  $^{13}\text{C}$  NMR (75 MHz,  $\text{CDCl}_3$ )  $\delta$  200.4, 200.1, 161.9, 141.3, 130.9, 122.8, 120.5, 116.1, 90.9, 88.5, 18.3, 18.0; HRMS ( $\text{Cl}^+$ ) calcd for  $\text{C}_9\text{H}_8\text{O}_2\text{FCl}_2$ : 236.9885, found 236.9883.

**2-Fluoro-1-(2-hydroxy-5-methylphenyl)propan-1-one (2a).** The same procedure as above was followed. The crude oil was purified by flash chromatography (96:4 hexanes/EtOAc) affording **2a** as a beige

solid.  $^1\text{H}$  NMR (300 MHz  $\text{CDCl}_3$ )  $\delta$  11.7 (s, 1H), 7.52 (s, 1H), 7.33 (dd, 1H), 6.93 (d, 1H), 5.76 (dq, 1H), 2.31 (s, 3H), 1.69 (dd, 3H);  $^{13}\text{C}$  NMR (75 MHz,  $\text{CDCl}_3$ )  $\delta$  201.3, 201.0, 161.2, 138.3, 129.3, 128.3, 118.5, 116.3, 89.8, 87.4, 20.5, 18.7, 18.4; HRMS ( $\text{Cl}^+$ ) calcd for  $\text{C}_{10}\text{H}_{13}\text{O}_2$  165.0916, found 165.0915.

**2-Fluoro-1-(2-hydroxy-5-nitrophenyl)propan-1-one (2c).** To a  $-78$  °C solution of 1.0 M sodium bis(trimethylsilyl)amide (14.0 mL, 14.0 mmol) in a three-neck flask fitted with an addition funnel was added 1-(2-hydroxy-5-nitrophenyl)propan-1-one (**4c**) (0.870 g, 4.46 mmol) dissolved in THF (9.0 mL) dropwise. The solution stirred for 90 min. at  $-78$  °C under argon, and then chlorotrimethylsilane (2.0 mL, 15.7 mmol) dissolved in THF (2.0 mL) was added dropwise. The resulting solution was mixed for 1 h at  $-78$  °C and then allowed to warm to rt for 1 h. Solid *tert*-butyl alcohol (1.2 g, 16 mmol) was quickly added to quench excess base, and the solution was transferred via cannula to Selectfluor (1.95 g, 5.50 mmol) dissolved in acetonitrile (50 mL) and trifluoroacetic acid (0.150 mL). (Note: Selectfluor is difficult to dissolve at rt even with prolonged sonication. The addition of trifluoroacetic acid assists in dissolving the reagent.) The combined solutions were mixed for 1 h at rt, and then tetrabutylammonium fluoride trihydrate (5.63 g, 17.8 mmol) was added, turning the solution bright yellow. After 30 min,  $\text{H}_2\text{O}$  was added (100 mL) and the solution stirred for 14 h. The layers were separated, and the aqueous phase was acidified with concentrated HCl (5 mL) and extracted with EtOAc ( $3 \times 50$  mL). The combined organics were washed with brine (75 mL), dried over  $\text{Na}_2\text{SO}_4$ , vacuum filtered, and concentrated by rotary evaporation at 40 °C. The heavy orange liquid was purified by flash chromatography (elution gradient from 9:1 hexanes/EtOAc to 1:1 hexanes/EtOAc, followed by a purge with 98:2 EtOAc/AcOH), providing 0.665 g (70%) of **2c** as an off-white solid:  $^1\text{H}$  NMR (300 MHz,  $\text{CDCl}_3$ )  $\delta$  12.3 (s, 1H), 8.79 (d, 1H), 8.32 (dd, 1H), 7.09 (d, 1H), 5.78 (dq, 1H), 1.71 (dd, 3H);  $^{13}\text{C}$  NMR (75 MHz,  $\text{CDCl}_3$ )  $\delta$  201.4, 201.1, 167.6, 139.6, 131.4, 126.8, 119.7, 115.5, 90.7, 88.3, 18.1, 17.8; HRMS ( $\text{Cl}^+$ ) calcd for  $\text{C}_9\text{H}_7\text{NO}_4\text{F}$  214.0516, found 214.0516.

**Method of  $\text{p}K_a$  Determination in Acetonitrile.** The  $\text{p}K_a$  values of the phenolic hydroxy groups of **1** in acetonitrile were determined by measuring relative acidities using a UV-vis spectrophotometric titration technique.<sup>31</sup> At first, the acid to be measured (HA) and a reference acid (HR) with known  $\text{p}K_a$  were titrated separately to obtain the spectra of the neutral (HA and HR) and deprotonated ( $\text{A}^-$  and  $\text{R}^-$ ) forms of both acids at known concentrations. Then, a solution containing the two acids was titrated with a transparent base. During the titration, 10 to 20 spectra at different acidities after each addition of a small amount of the base were recorded, including those where both acids were in neutral or fully deprotonated form. The spectra of the mixed acid solution titration were resolved to the individual spectra of HA,  $\text{A}^-$ , HR, and  $\text{R}^-$  by multiple linear regression by using Origin (Microcal Software, Inc.). Thus, the value of  $[\text{HA}][\text{R}^-]/[\text{A}^-][\text{HR}]$  was obtained. Since both acids were in the same solution, the value of activity ratio  $a_{\text{HA}}a_{\text{R}^-}/a_{\text{A}^-}a_{\text{HR}}$  should be almost the same as the concentration ratio  $[\text{HA}][\text{R}^-]/[\text{A}^-][\text{HR}]$ . The  $\text{p}K_a$  of HA was readily calculated with the equation of  $\text{p}K_a(\text{HA}) = \text{p}K_a(\text{HR}) + \log([\text{HA}][\text{R}^-]/[\text{A}^-][\text{HR}])$ . From each titration experiment, the  $\text{p}K_a$  was determined as the mean of 5 to 10 values from the spectra where both  $[\text{HA}]/[\text{A}^-]$  and  $[\text{R}^-]/[\text{HR}]$  were not extremely large or small (values between 0.2 and 0.8 were preferred). To measure the concentration correctly, the difference between the two acids'  $\text{p}K_a$ s should be less than two units, and the two acids and their deprotonated forms should have apparent differences in their absorbance spectra; otherwise, the mixed spectra could not be resolved properly. By this technique, it is not necessary to know the accurate concentrations of the acids. Further, the results were not

(30) Powell, M. T.; Porte, A. M.; Reibenspies, J.; Burgess, K. *Tetrahedron* **2001**, *57*, 5027–5038.

(31) Leito, I.; Kaljurand, I.; Koppel, I. A.; Yagupolskii, L. M.; Vlasov, V. M. *J. Org. Chem.* **1998**, *63*, 7868. Leito, I.; Rodima, T.; Koppel, I. A.; Schwesinger, R.; Vlasov, V. M. *J. Org. Chem.* **1997**, *62*, 8479.



sensitive to the presence of small amounts of other solvents in acetonitrile, because the solvent impurities have similar effects on both acids.

All titrations were done in a 1 cm light path UV–vis cell equipped with a silicone septum. A solution of 0.3 M tetrabutylammonium hydroxide in methanol was used as the base for the titrations. Solutions of **1** were made in anhydrous acetonitrile with 1% methanol by volume in 0.04 to 0.15 mM so that the maximum absorbance between 300 and 600 nm was in the range of 0.8 to 1.4. Titrations of **1** in pure acetonitrile with the base solution in methanol did not give satisfying results because the spectra of deprotonated **1** were very sensitive to the solvent composition change during the titrations, even though only less than 0.1 vol % of the methanol solution was needed to fully deprotonate the acids. In the presence of 1% methanol, the spectra change caused by the addition of methanol in the base solution was negligible. **1a–c** were titrated by using 4-bromophenol as a reference acid, which has a  $pK_a$  of 25.53 in acetonitrile.<sup>32</sup> 4-Nitrophenol ( $pK_a = 20.53$ )<sup>32</sup> was used as the reference for **1d**, and **1d** was used as the reference for **1e**. The error of the measurements was within  $\pm 0.06$   $pK_a$  units.

**Method of  $pK_a$  Determination in Methanol/Water (4:1 v/v).** The  $pK_a$  values of the phenolic hydroxy groups of **1** in methanol/water (4:1 v/v) were determined by a slightly modified literature method.<sup>33</sup> In a two-neck flask equipped with septum and a glass electrode, 100 mL of methanol/water (4:1 v/v) solution of **1** in the concentration range of 0.05 to 0.15 mM, which was adjusted to give a maximum absorbance of around 1, was titrated by 0.5 M NaOH solution in the same solvent. After each addition of base aliquots, pH values were read, and UV–vis spectra were recorded by transferring samples of 1.0 mL of the

solution through a Hamilton gas-tight syringe into a UV–vis cell precharged with argon. Typically, around 10 spectra, including those where the titrant was in neutral (HA) and fully deprotonated ( $A^-$ ) forms, were measured for each titration experiment. The absorbance spectra were resolved into individual spectra for HA and  $A^-$  by multiple regression using Origin (Microcal Software, Inc.). Thus, the values of  $[A^-]/[HA]$  at each pH were obtained. Plotting  $[A^-]/[HA]$  to  $1/[H^+]$  gave  $K_a$  as the slope.

**Kinetics Measurement for the H/D Exchange.** Solutions of 20 mM **1** or **2** with buffer in deuterated solvents in NMR tubes were prepared. The rate of the H/D exchange reaction of **1** or **2** was measured by  $^1H$  NMR monitoring the decreasing  $ArCOCH_3$  peak. In most cases, three to six data points were collected in the range of 10–60% conversion for each sample. The conversion ratios were calculated by comparison of the integral of the  $ArCOCH_3$  signal with those of inert  $ArH$  or  $ArOMe$  protons. The data fit well with a first-order kinetics equation. The error of the pseudo-first-order rate constants was estimated to be less than 15%.

For the studies in  $CD_3OD/D_2O$  (4:1 v/v), the samples were buffered with 100 mM of imidazole/imidazolium chloride at pD 5.83 (pH meter reading without correction), and the source of deuterium for the H/D exchange was from the deuterated solvents. For the studies in  $CD_3CN$ , the samples were buffered with 150 mM imidazole- $d_2$  and 150 mM imidazolium- $d_3$  triflate and the deuterium source was the deuterated buffer.

**Acknowledgment.** We gratefully acknowledge support from the National Institutes of Health for the funding of this project (GM 65515).

JA0306011

(32) Vorokov, M. G.; Kashik, T. V.; Ponomareva, S. M.; Kuliev, F. A.; Farzaliev, V. M. *J. Gen. Chem. USSR* **1979**, *49*, 1813.  
(33) Alves, K. B.; Bastos, M. P.; do Amaral, L. *J. Org. Chem.* **1978**, *43*, 4032.